Decentralized Frequency Control of AC Microgrids: an Estimation-Based Consensus Approach

Yousef Khayat, *Student Member, IEEE,* Rasool Heydari, *Member, IEEE,* Mobin Naderi, Tomislav Dragicevic, *Senior Member, IEEE,* Qobad Shafiee, *Senior Member, IEEE,* Mohammad Fathi, Hassan Bevrani, *Senior Member, IEEE* and Frede Blaabjerg, *Fellow, IEEE*

***Abstract*—In this paper, a decentralized secondary control (SC) based on the active power estimation (APE) is presented. This achievement is realized by employing the unique feature of frequency as a global variable in autonomous AC microgrids (MGs). The APE is merely based on the droop coefficient of $P-\omega$ characteristics. The decentralized SC, utilizing a consensus protocol, restores the MG frequency to the nominal value while maintaining accurate power-sharing of the droop mechanism. The consensus protocol is estimation-based and does not require communication infrastructure. In addition to the proposition of stability analysis method, experimental results with four distributed generation units (DGUs) also verify the effectiveness of the proposed SC structure.**

***Index Terms*—Active power estimation, communication free control, consensus protocol, frequency regulation, microgrid, secondary control.**

I. Introduction

Today, microgrids (MGs) are introduced as a promising solution for future power systems. They can be operated in the grid-connected or islanded modes. A hierarchical control strategy is introduced to satisfy the operational objectives in the islanded MGs. The primary control, secondary control (SC), MG emergency/central control (MGCC), and global control are the main layers in this hierarchical scheme [1]. The primary control layer includes three main control loops: current control, voltage control, and droop control mechanism. This cascaded control, however, can also be avoided by some advanced control techniques [2]. This control layer guarantees the MG voltage and frequency stability.

Although the droop strategy ensures (active) power sharing, it makes steady state errors in the voltage amplitude and frequency. The SC of the MG is introduced to restore the frequency and voltage amplitude to the nominal values while assuring proportional power sharing among DGUs [3], [4] precisely. The SC of the MGs can be affected by communication network (CN) uncertainties and cyber-attacks [5]. Though vital rules of the CN are undeniable in hierarchical control plat-form of the MG, reducing the use of CN infrastructure in the SC layer can improve the reliability of the overall system [6], [7].

Centralized, distributed, and decentralized are three main architecture for the SC implementation. The performance of the centralized SC is highly depended on the point-to-point communication among all DGUs and suffers from single point of failure, which leads to low reliable operation [8].

Recently, distributed SC has been proposed to reduce the malicious effect of CN failures such as time delays and data drop-out [9]–[12]. As DGUs in the MG are spatially distributed and heterogeneous, distributed control structures are promising approaches to improve the MG reliability. Compared to the centralized architecture, distributed SC architecture provides higher reliability as well as more scalability by applying a sparse CN. Averaging distributed SC [13]–[16] and consensus based SC [17]–[20] policies are two main distributed SC architectures. In the averaging distributed SC architecture, each DGU measures its required data (e.g. voltage and frequency) and transmits them to all the other DGUs in the MG. By averaging the received data from other DGUs, the SC signal is built. In this structure, the MGCC for the SC is not needed. Furthermore, the required communication links decreased. In the consensus based SC structures, the CN is reduced more by transferring the required data just among the neighbour DGUs. Stability and robustness of this control approach is proved in [9], [11], [15], [21].

Although the presented distributed architectures reduce the required CN, and consequently enhance the system reliability, CN infrastructure failure, data drop-out or even time delays degrade the performance of this control structure. Furthermore, for the MG with many DGUs, the presented distributed structures are often not sufficient since the CN topology may be very complex and dynamic.

Therefore, to reduce the CN dependency, event-triggered based SC methods are introduced to decrease the information exchange among DGUs, and consequently required CN bandwidth [22]. In this structure, instead of continuous data transmission among DGUs or MGCC, the required frequency and voltage data can be shared when an event is triggered or a criteria is satisfied [23], [24]. Event-triggered, time-triggered, and self-triggered sampling methods are three main approaches to realize event-based SC. Although this approach is increasingly employed in the recent SC architectures, it still requires the constant monitoring of the state(s) to determine the current MG performance. Moreover, complex design feature of the event-triggered based SC structures is the main drawback of

Y. Khayat, M. Naderi, Q. Shafiee, M. Fathi, and H. Bevrani are with the Department of electircal Engineering, University of Kurdistan, Sanandaj, Iran, email: y.khayat@eng.uok.ac.ir, m.naderi@eng.uok.ac.ir, q.shafiee@uok.ac.ir and bevrni@uok.ac.ir).

R. Heydari is with Electrical Engineering, Mads Clausen Institute, University of Southern Denmark, Odense, DK, 5230, Denmark, e-mail: (rah@mci.sdu.dk)

T. Dragicevic and F. Blaabjerg are with the Department of Energy Technology, Aalborg University, Aalborg, DK, 9220, Denmark, e-mail: (tdr@et.aau.dk, fbl@et.aau.dk).

these approaches.

Communication-free decentralized SC architectures have recently been presented in the literature to eliminate the required CN in the SC level of the hierarchical MG control [25]–[28]. In this SC architecture, the CN is not used for the voltage and frequency restoration in the MG.

Washout-filter based decentralized SC methods have been presented in [29]–[31]. A simplified band-pass washout filter is introduced in [30] to restore the voltage and frequency of the MG. The proposed band-pass washout filter for the SC in [30] is realized by cascading a high-pass filter and a low-pass filter. In [32], a second-order washout filter based power sharing approach for uninterruptible power supply (UPS) with stability analysis is introduced. Though washout-filter based SC approaches are fully communication free, but they mainly suffers from long restoration time and sluggish dynamic performance. Estimation-based decentralized SC has been introduced to control the MG voltage and frequency in [33] and [34], which nonlinear and Luenberger-like observers with complex calculation is applied. In [35], only local signals are applied to design a secondary controller according to a time-dependent protocol without any CN. However, the proposed method in [35] only control the frequency without accurate power sharing, with slow response for frequency restoration. Furthermore, a number of decentralized control methods have been introduced in [36]–[38], However, these methods still need the CN infrastructure.

In this paper, a consensus-based SC is proposed to restore the MG frequency and share the active power among DGUs, employing active power estimation (APE). The stability analysis of the frequency-active power dynamics of the whole system is presented in the form of a multi-input single-output (MISO) transfer function. In addition, the control parameters of the consensus protocol is determined to keep the system stable. In contrast to the existing communication-free SC approaches, our proposed method provides the following salient features:

- Opposed to the decentralized methods presented in [33], [34], which need a complete knowledge of the MG topology to estimate the variables, the proposed method takes advantage of the unique feature of the frequency in islanded MGs as a global variable in steady state to achieve APE.
- Comparing with most of the distributed secondary control approaches [7], the proposed approach employs a communication-less structure, which enhances the reliability of the MG, due to the lack of CN failures and cyber-attacks [39].
- Unlike the introduced decentralized methods in [25], [26], [35], the proposed solution enhances the reliability of the MG, by utilizing a consensus approach.

The reminder of this paper is organized as follows. Section II proposes three main SC architectures based on the required CN, and function of the SC in a hierarchical control structure of the MG. In Section III, active power estimation with its remarks are explained. The proposed decentralized SC approach is presented in Section IV. In Section V, experimental verification is provided to show the effectiveness of the proposed SC strategy. Finally we conclude the remarks of the study in Section VI.

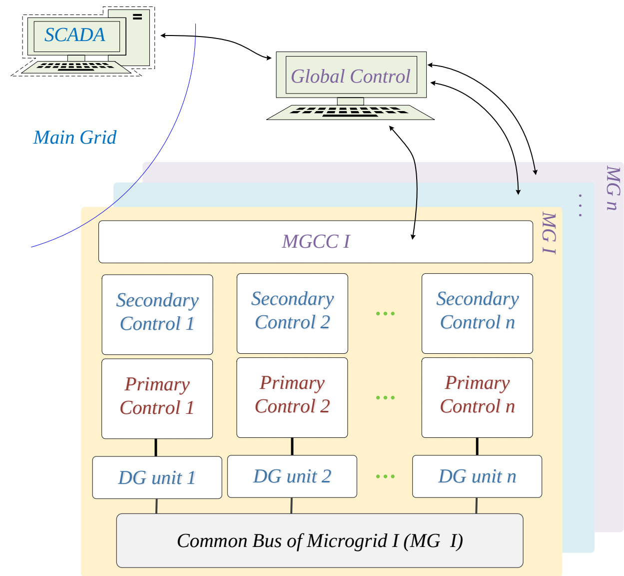

Fig. 1. General schematic of MG's hierarchical control.

II. Secondary Control Architectures and Functions in Hierarchical Control of MGs

In hierarchical control platform of MGs,as shown in Fig. 1, the SC is placed between the local (primary) control and the MGCC. The MGCC and global control, which are introduced in a number of literature as tertiary layer, have an important role to meet optimization needs of operational constraint in both the grid-connected and islanded modes of an MG by a reliable and proper manner/control pattern. Optimal unit commitment, critical and non-critical load servicing and DGU plug-and-play, emergency load-shedding, and initialization of protection strategies are categorized as the main objectives of the MGCC. Likewise, economic dispatch of networked MGs with respect to balance demand-generation is determined by the global control. Accurate details on MGCC and global control duties, functions, and real-life examples can be found in Chapters 5 and 11 of [1].

A general scheme which illustrates various control response time-scales in a conventional power systems is illustrated in Fig. 1(a). Inertia response (IR), primary control (PC) response, SC response, tertiary control (TC) control, and generator rescheduling are the main control loops in a convectional power system [40]. Unlike the conventional power systems, power electronic interfaces are mainly employed in MGs to converse renewable energies. However, power electronic interfaces are mainly fast enough to provide an appropriate control response to a disturbance (such as load/generation changes or contingencies). The activated power by DGUs has operational limitations such as the nominal power or over-current of the power electronic switches [41]. Accordingly, a hierarchical control scheme for MGs have been presented, in which the time-scale of the control responses can be shown

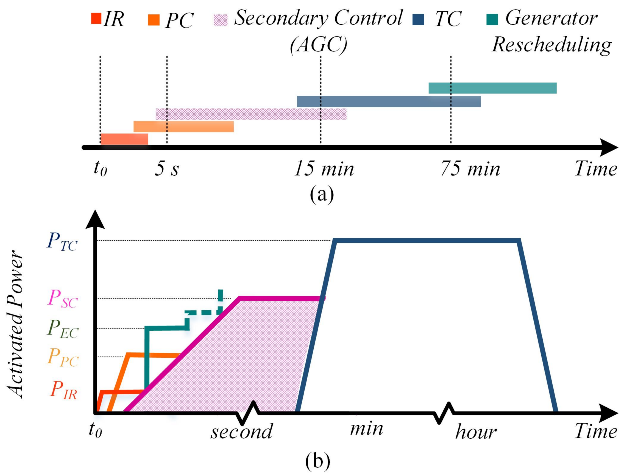

Fig. 2. (a) A typical time-scale of frequency-related dynamics in conventional power systems, and (b) activation of frequency control loops following a disturbance at t_0 in an MG [39].

as Fig. 1(b). The IR, PC, SC, emergency control (EC), and TC time scale range for an MG are shown in Fig. 1(b). By applying a disturbance at time t_0, control loops mostly have a time-range as depicted in Fig. 1(a), while, both time-scale and the amount of activated power need to be considered in an MG. The SC is an interface control between the primary control as a local control for each DGU and the MGCC or tertiary control for all DGUs. It can be realized with or without a communication infrastructure. It is worth to note that even with an SC layer with no CN, a general CN infrastructure is needed for the MGCC functionalities such as black-start process of DGUs or other functions of global control. In the following, as illustrated in Fig. 3, three main architectures on how an SC can be implemented, and then the functions of the SC are explained.

A. Secondary Control Architectures

1) Centralized control framework: In this control structure, a central controller is utilized to achieve global controllability and compensate for the MG frequency and voltage deviations in steady state. Therefore, a CN is required to transmit data between the central controller and DGUs. The principal merit of this architecture is strong observability and controllability of the whole MG. However, this structure relies on the single point of the communication link. Therefore, any failure on the CN or central controller leads to collapse on the SC level.

2) Distributed control framework: In this control structure, the SC level is implemented locally like the primary control level, and the communication link at the upper level transmit the required data (e.g. frequency and voltage amplitude) among DGUs. In this approach, the control unit of each DGUs *talk* to the other DGUs through digital communication, hence, the shared required data is minimized and the MGCC is not employed. Receiving the required data from one or more DGU makes the system more reliable. Advanced communication technologies such as Zigbee and WiFi and also new transfer algorithms such as consensus, peer to peer, OpenFMB, and

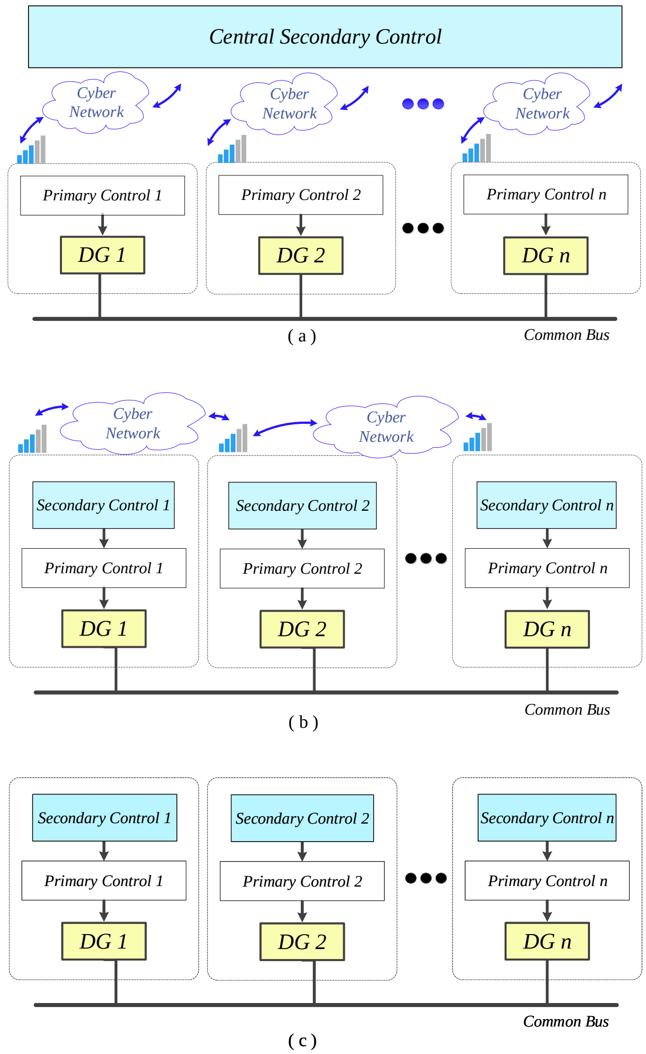

Fig. 3. Secondary control architectures: a) centralized secondary control, b) distributed secondary control, and c) decentralized secondary control.

gossip have been implemented in the distributed control structure to enhance the system performance. The primary challenge of this structure is to satisfy all the control objectives, which make the system design more complex. Furthermore, the distributed SC architecture still relies on the CN in infrastructures.

3) Decentralized control framework: This approach is a communication-free control structure. In this manner, the SC is implemented locally and also use only the local measurements or estimated variable of the neighbor units to achieve the proper controllability in the MG. Therefore, by applying the accurate estimation, the proper signal is sent to the primary controller to compensate for the voltage and frequency deviations of the MG. Although data transmission among DGUs and communication link is eradicated in this manner, the complex calculation and estimation are required. Fig. 3 shows a comprehensive schematic among centralized, distributed and decentralized SC architecture, regarding communication network requirement. As it can be seen from Fig. 3(c), in the decentralized SC architecture, the SC is implemented as a local controller and the CN is eliminated while the MG maintained stable.

B. Secondary Control Functions

At the outer primary control level, the droop control is applied to tuning the amplitude of the voltage and frequency locally. It also shares the active and reactive power among DGUs, in a decentralized manner, based on their droop gains, m_i, as follows:

$$\omega_i^d = \omega^* - m_i.P_i \,, \tag{1a}$$
$$v_i^d = v^* - n_i.Q_i \,, \tag{1b}$$

where m_i and n_i are droop coefficients for the frequency and voltage tuning respectively, ω^* and v^* are the reference frequency and voltage, while P_i and Q_i are filtered active and reactive powers respectively.

$$P_i = G_{\text{LPF}}(s)p_i \qquad p_i = v_{odi}i_{odi} + v_{oqi}i_{oqi} \tag{2a}$$
$$Q_i = G_{\text{LPF}}(s)q_i \qquad q_i = v_{oqi}i_{odi} + v_{odi}i_{oqi} \tag{2b}$$

where $G_{\text{LPF}}(s) = \omega_c(s+\omega_c)^{-1}$ is a low-pass filter with cutoff frequency ω_c applying for measuring active and reactive power. Moreover, i_{oi} and v_{oi^d} are the instantaneous output current and voltage of DGU$_i$ in $d-q$ frame. In (1), ω_i^d and v_i^d are references for angular frequency and voltage amplitude, which are sent to the inner voltage/current control loops. Any change in P_i and Q_i at (1) will change the value of ω_i^d and v_i^d, which leads to the steady state error.

In order to eliminate the steady state errors and enhance the power quality of the MG, the SC runs with appropriate functions to compensate for the ω_i^d and v_i^d deviations, while the stability of power sharing, voltage, and frequency of MG should be remained. Mathematically, the SC framework satisfies the following expressions:

$$\lim_{t\to t_f} \omega_i(t) = \omega^* \,, \tag{3a}$$
$$\lim_{t\to t_f} v_i(t) \approx v^* \,, \tag{3b}$$

where (3a) and (3b) represent the frequency restoration and voltage regulation in a finite time, such as t_f, respectively. It is worth to highlight that since the voltage is a local variable in the system, accurate voltage regulation and reactive power sharing cannot be obtained together using the droop mechanism in (1b). In this paper, we only focus on (3a) and assume that the $Q-v$ droop mechanism regulates the v_i for the DGUs. In order to share the active power appropriately and (3a) satisfactory, the SC adds a correction term to (1a) as follows:

$$\omega_i = \omega^* - m_i.P_i + \delta\omega_i \,, \tag{4}$$

where, $\delta\omega_i$ is the control signal provided by the SC and ω_i is the restored frequency of DGU$_i$.

III. Proposed Secondary Control

In the proposed control structure, firstly, the active power estimation is presented. To this end, the unique feature of the frequency in MGs is employed, which is a global variable. Then, the proposed consensus method will be presented, it will be shown that each SC is fully decentralized and communication-free unless in emergency situations determined by the MGCC. In the proposed SC, the concept of adjacency matrix on graph theory has been employed, which is briefly explained in the following subsection.

A. Active Power Estimation

In this section, a simple method for APE of neighbour DGU$_j$ in the location of DGU$_i$ is proposed, where $\{i, j \in N\}$ and N is the number of DGUs. As mentioned before, the estimation is exclusively based on $P-\omega$ coefficients. Since the frequency in autonomous MGs is a global variable, in the steady state and normal operation of the DGUs under demand/generation operation, the APE of the neighbour DGUs can be denoted as given below:

$$\hat{P}_j = \frac{\omega^* - \omega_i^d}{m_j} \,, \tag{5}$$

where, $\hat{P}_j$ is the APE of DGU$_j$ in DGU$_i$.

It is worth to note that the control command for plug-and-play (PnP), connection or disconnection a DGU to the MG based on a pre-planned or unintentional scenario, will be given by the MGCC or from the tertiary control level. The estimated power $\hat{P}_j$ at (5) is true unless a control signal from the MGCC, accidentally or intentionally, orders to DGU$_j$ to plug-off. Obviously, in this situation $\hat{P}_j = 0$.

B. Adjacency Matrix Expression

An adjacency matrix $\mathbf{A} = [a_{ij}] \in R^{N\times N}$ shows the neighbourhood status of DGUs. Unlike the networked control systems that a_{ij} shows the direction and the communication weights, here it shows just the neighborhood status, i.e., if DGU$_i$ is a neighbour of DGU$_j$ then $a_{ij} = a_{ji} = 1$, otherwise $a_{ij} = a_{ji} = 0$. More information about the description of a_{ij} for a system, direction and weighting values, and the guarantee of an eventual convergence of the control variable to the desired value are addressed in [42]. It is worth clarifying that disconnection of DGU$_j$ as a neighbor of DGU$_i$ also makes $a_{ij} = a_{ji} = 0$.

The basic preliminary for distributed cooperative control is the CI network, so it is reasonable to represent a brief review on concepts about modelling and networks as follows. In a MG system with N DGUs, each characterized by a state variable $x_i(t) \in \mathbb{R}^n$ subject to a control input $u_i(t) \in \mathbb{R}^n$ given as follows:

$$\dot{x}_i(t) = Ax_i(t) + Df(t, x_i(t)) + Bu_i(t) \tag{6}$$

where $i = 1, 2, ..., N$.

Cooperative control means to implement a distributed protocol by employing the CI such that the state of each DGU can reach agreement as $t \to \infty$; that is

$$\lim \|x_i(t) - x_j(t)\| = 0, \quad \forall\ i,\ j = 1, 2, ..., N. \tag{7}$$

The communication network of a MAS can be expressed by a directed graph (digraph) $\mathcal{G}$, which it is usually modelled as $\mathcal{G} = (\mathcal{V}_\mathcal{G}, \mathcal{E}_\mathcal{G}, \mathcal{A}_\mathcal{G})$ with a nonempty finite set of $\mathcal{N}$ nodes $\mathcal{V} = \{\nu_1, \nu_2, ..., \nu_N\}$, a set of edges or arcs $\mathcal{E}_\mathcal{G} \subset \mathcal{V}_\mathcal{G} \times \mathcal{V}_\mathcal{G}$, and the associated adjacency matrix $\mathcal{A}_\mathcal{G} = [\alpha_{ij}]_{N\times N}$. In a MG, DGUs are considered as the nodes of the communication digraph, i.e., $\mathcal{V}$, and the edges of the corresponding digraph $\mathcal{G}$ of the communication network denote the communication links.

C. Control Protocol

Firstly, in each control unit, active power of neighbour DGUs will be estimated. These APE values will be checked with an MGCC protection logical switch to check the PnP command situation. Then, the APE values are used in a consensus control protocol. Accordingly, the frequency SC unit at DGU$_i$ updates its value continuously based on

$$\delta u_{\omega i} = m_i P_i(t) + \int_0^t \sum_{j\in N_i} c\, a_{ij} \left(m_j \hat{P}_j(\tau) - \delta u_{\omega i}(\tau)\right) d\tau \,, \tag{8}$$

where the consensus coupling gain c is the design gain. Accurate details for the optimal design of coupling gains on the consensus protocols can be found in [43]. An implementation diagram of the proposed controller is illustrated in Fig. 4.

IV. Stability Analysis

In this section, a stability analysis of the proposed SC is presented. Fig. 5(a) shows a simple equivalent model of a DGU connected to the point of common coupling (PCC) in the MG [44]. The generated active power by the DGU can be obtained as follows

$$p_i = \frac{x_{eqi}(V_i V_b \cos(\varphi_i) - V_b^2) + r_{eqi} V_i V_b \sin(\varphi_i)}{x_{eqi}^2 + r_{eqi}^2}, \tag{9}$$

where, V_i is the output voltage amplitude of the DGU$_i$, V_b is the voltage amplitude in the PCC, and φ_i is the voltage phase difference between the DGU$_i$ and the PCC. x_{eqi} and r_{eqi} are coupling inductance and resistance between the DGU$_i$ and the PCC. For an inductive line, the active power p_i can be simplified as:

$$p_i \approx \frac{3V_i V_b}{2x_{eqi}} \sin(\varphi_i), \tag{10}$$

By a logical assumption $\sin(\varphi_i) \approx \varphi_i$, the micro-scale transferred power from the DGU$_i$ can be rewritten as

$$p_i \approx \frac{3V_i V_b}{2x_{eqi}} \varphi_i = \frac{3V_i V_b}{2x_{eqi}} \frac{\omega_i}{s} = G_{\omega pi} \cdot \omega_i. \tag{11}$$

Mainly, a low-pass filter is employed in power measurement units, as

$$P_i = \frac{\omega_c}{s + \omega_c} p_i. \tag{12}$$

where ω_c stands for the cut-off frequency of the low-pass filter. Accordingly, based on the Fig. 5, $\delta\omega_i$ can be rewritten as follows:

TABLE I. Parameters of the Test System

Electrical Parameters		
Parameters	Symbol	Value
Output voltage of rectifier	V_{DC}	650 V
Nominal voltage magnitude	V_i	325 V
Nominal Frequency	f	50 Hz
Switching Frequency	f_s	10 kHz
Capacitance of LCL filter	C_f	25 μ F
Input / output inductance of LCL filter	L_i / L_o	1.8 mH
Load 1	Z_1	43 Ω , 0.3 H
Load 2	Z_2	124 Ω , 0.1 H
Load 3	Z_3	124 Ω , 0.1 H
Inner loop coefficients and other control Parameters		
Control Parameters	DGU: 2 and 4	DGU: 1 and 3
$P-\omega$ droop coefficient	0.001 rad/W.s	0.002 rad/W.s
$Q-v$ droop coefficient	0.005 V/VAr	0.01 V/VAr
Current integral / proportional terms	1000 / 0.5	1000 / 0.5
Voltage integral / proportional terms	120 / 0.05	120 / 0.05
Control design gain c	200	200

$$\delta\omega_i = m_i P_i + \frac{a_{ij} \cdot c}{s} (m_j \hat{P}_j - \delta\omega_i) \,,$$

then,

$$\delta\omega_i = \frac{s}{s + a_{ij} \cdot c} m_i P_i + \frac{a_{ij} \cdot c}{s + a_{ij} \cdot c} m_j \hat{P}_j \,. \tag{13}$$

In order to find the transfer function for the frequency analysis (ω_i) of DGU$_i$, (13) is inserted in (4) as follows:

$$\begin{aligned}\omega_i &= \omega^* - m_i P_i + \frac{m_i \cdot s}{s + a_{ij}c} P_i + \frac{m_j \cdot s}{s + a_{ij}c} \hat{P}_j \\ &= \omega^* - \frac{m_i \cdot \omega_c}{s + \omega_c} G_{\omega pi} \cdot \omega_i + \frac{m_i \cdot s}{s + a_{ij}c} \frac{\omega_c}{s + \omega_c} G_{\omega pi} \cdot \omega_i \\ &\quad + \frac{m_j \cdot s}{s + a_{ij}c} \hat{P}_j.\end{aligned} \tag{14}$$

Then,

$$\omega_i = \omega^* - \overbrace{\frac{m_i \cdot \omega_c \cdot G_{\omega pi}}{s + \omega_c} \frac{a_{ij}c}{s + a_{ij}c}}^{G_1} \cdot \omega_i + \overbrace{\frac{m_j \cdot s}{s + a_{ij}c}}^{G_{\delta\hat{P}}} \hat{P}_j \,. \tag{15}$$

Accordingly, the behaviour of ω_i can be achieved as:

$$\omega_i = (1 + G_1)^{-1} \omega^* + (1 + G_1)^{-1} G_{\delta\hat{P}} \hat{P}_j \,, \tag{16}$$

where, $(1 + G_1)^{-1} G_{\delta\hat{P}} \hat{P}_j$ can be regarded as a disturbance term. Obviously, (16) describes the dynamics of the system in a MISO manner, with two inputs and one output. To analyze the stability of the system in the presence of the proposed SC, all the poles of transfer functions ${}^{\omega_i}/_{\omega^*}$ and ${}^{\omega_i}/_{\hat{P}}$ must stay in the left-hand complex plane (LHP). A root locus analysis is shown in Fig. 6, for various amounts of the control parameter c in the presence of disturbance term ($a_{ij} = 1$). As it can be seen, only for $c > 150$ the system can be stable. However, by decreasing the power rating of the DGUs (i.e., increasing the droop coefficient m_i), the dominant poles of the system will be slowly damped.

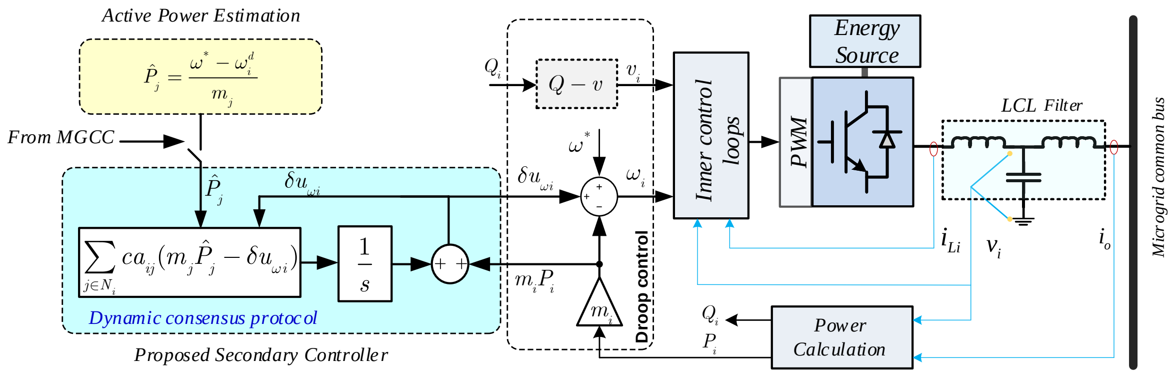

Fig. 4. Proposed communication-free secondary control.

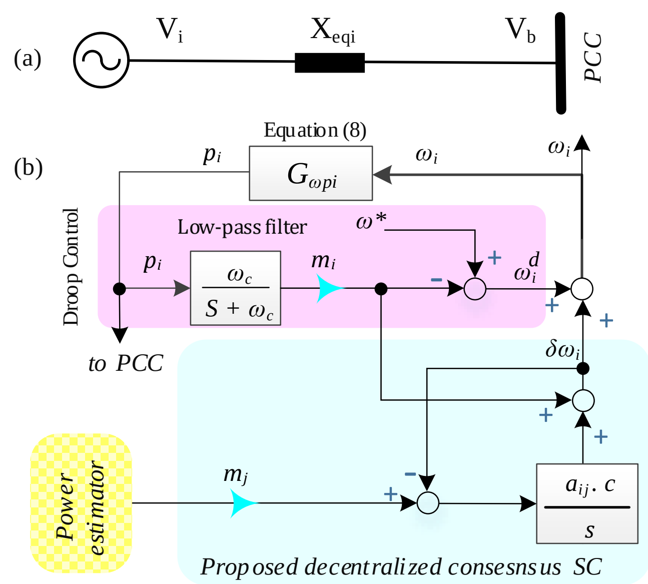

Fig. 5. Equivalent and dynamic models of a DGU connected to the PCC: (a) equivalent model of a DG connected to the PCC, (b) flow-graph model of a DGU and the proposed SC to close-loop stability analysis.

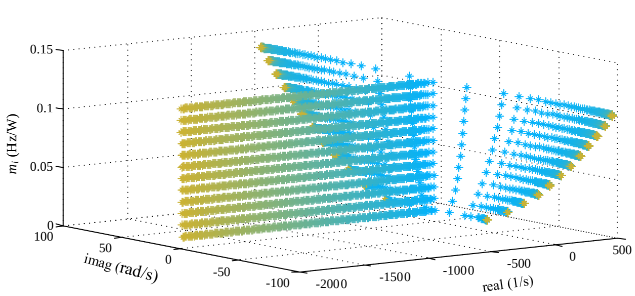

Fig. 6. Dominant closed-loop poles for various values of the control parameter c, and power rating of DGUs when $a_{ij} = 1$.

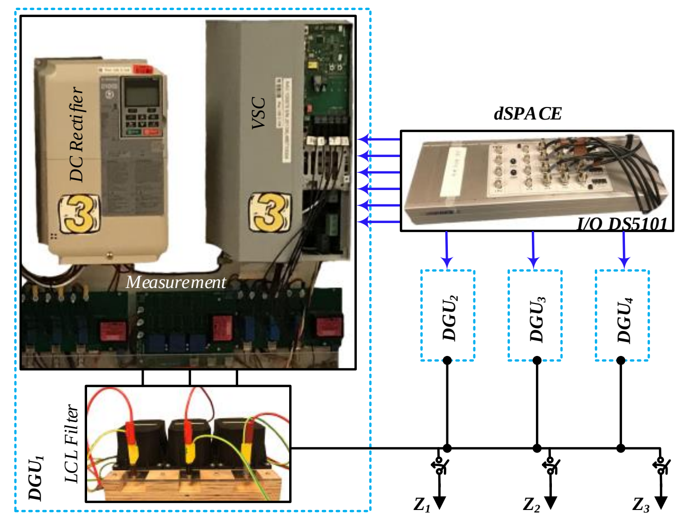

Fig. 7. Configuration of the studied MG with four DGUs.

V. Experimental Verification

The performance of the proposed solution is verified using a laboratory-scaled MG with the parameters given in Table I. The schematics of the experimental case study is shown in Fig. 7. To show the merits of the communication-free SC, an experimental test is carried out in the following scenarios.

A. Scenario 1: SC activation

The performance of the proposed communication-free SC is shown in Fig. 8, where, ω_i and P_i stand for the frequency and output active power of DGU_i, respectively.

As it can be seen, at $t = 1$ s, Z_1 is switched on and the $P - \omega$ droop tunes the frequency value, till $t < 6$ s that the proposed SC will be activated. When the proposed SC is applied at t=6 s, the frequency is restored to the nominal value, and also the active power sharing is remained proportionally shared.

B. Scenario 2: Load change

As shown in Fig. 9, when Z_2 is switched on, the frequency drops down and the active power is increased. Consequently,

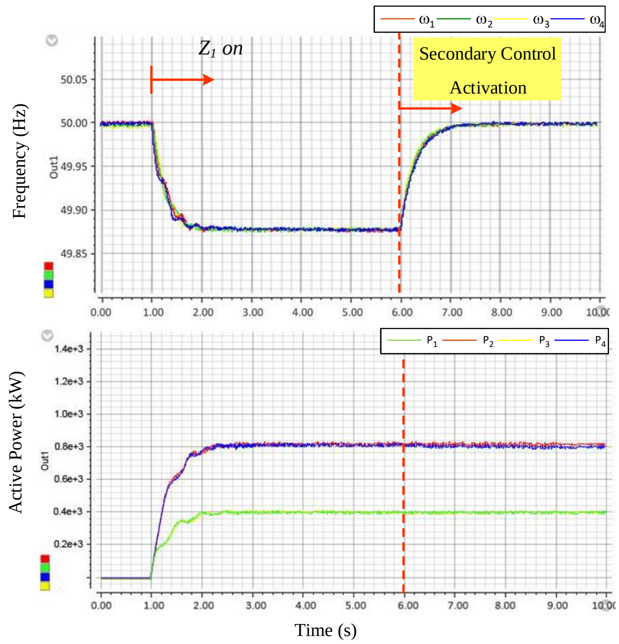

Fig. 8. Experimental results to compare the droop control and the proposed SC in Scenario 1.

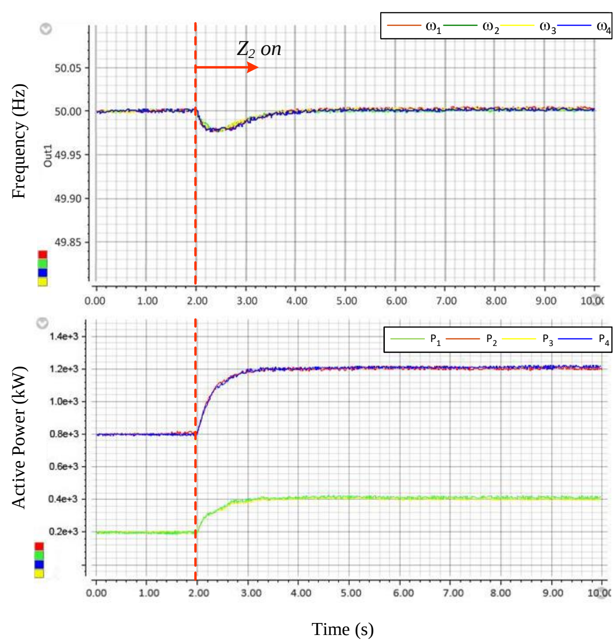

Fig. 9. Frequency restoration and active power sharing in the presence of load change in Scenario 2.

after the load change, the proposed SC restores the frequency to the nominal value.

C. Scenario 3: DGU Plug-off and load change

In this Scenario, DGU_2 is intentionally switched off as shown in Fig. 10. The excess active power demand is shared accurately among the remaining DGUs. Then, Z_3 is switched on as a disturbance, for the new structure of the MG. As it

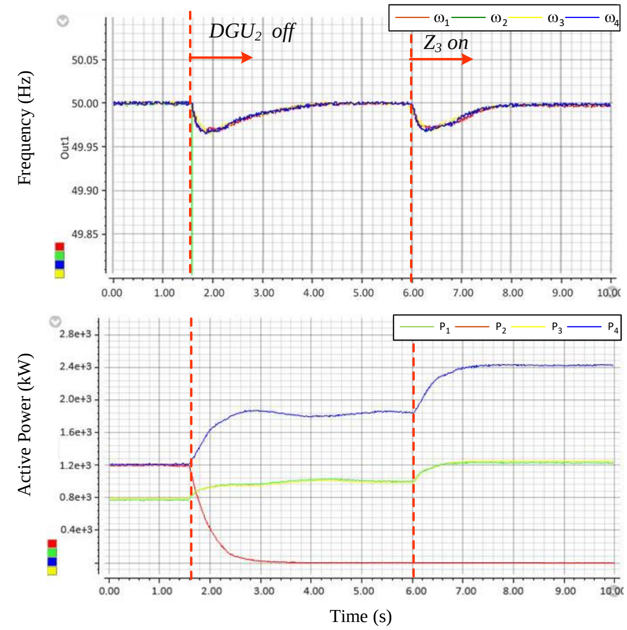

Fig. 10. Performance of the proposed SC in Scenario 3 (DGU plug-off and load change).

can be seen, retaining the frequency in the nominal value and accurate active power sharing among DGUs is achieved.

D. Scenario 4: A Comparison Study

To evaluate the proposed control structure performance, a distributed control architecture proposed in [45] is also implemented to serve as a benchmark. Fig. 11 shows the active power sharing comparison between the proposed decentralized control structure (Fig. 11(a)) and a distributed control architecture (Fig. 11(b)) [45] considering 500 ms communication link time delay. A frequent load change is applied at t=4.5 s and t=8 s. As the proposed control structure do not need the communication infrastructure, time delay or communication disturbances have no effect on the performance of active power sharing among DGUs, while the distributed control structure and obviously centralized control architecture relay on the transmitted data through communication infrastructure. As can be seen from Fig. 11(b), by applying 500 ms time delay, the active power sharing performance is degraded.

The same results are achieved for the frequency response. Fig. 12 shows the frequency control comparison between the proposed communication free control structure (Fig. 12(a)) and a distributed control architecture proposed in [45], (Fig. 12(b)) considering 500 ms communication link time delay. The communication deficiencies have no effect on the proposed control structure, while a small time delay degrades the frequency control performance of distributed control architecture as shown in Fig. 12(b).

VI. Conclussion Remarks and Future Works

This paper introduces a totally communication-free secondary control for the frequency restoration in the autonomous

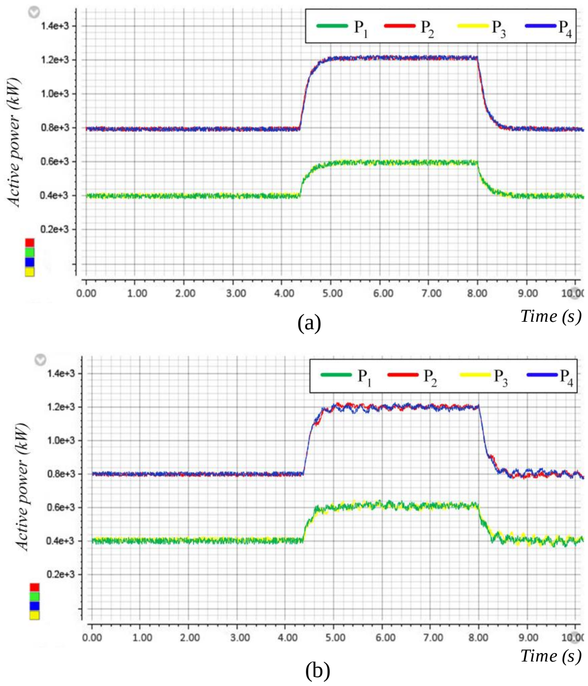

Fig. 11. Active power sharing performance comparison of (a) proposed decentralized control scheme versus (b) distributed secondary control introduced at [45] by considering communication delays effect.

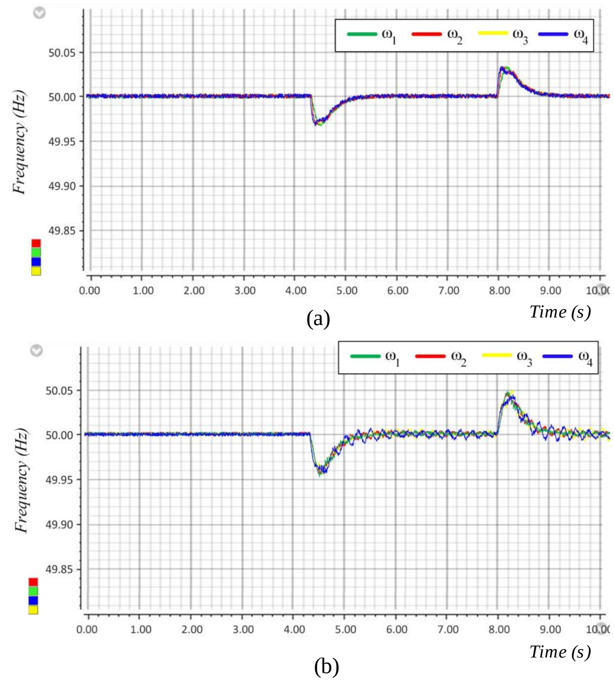

Fig. 12. Frequency control performance comparison. (a) The proposed decentralized control scheme versus (b) distributed secondary control introduced at [45] by considering communication delays effect.

microgrids (MGs). A consensus-based solution employing active power estimation is utilized which guarantees stability of the system while the required communication network infrastructure is eliminated at the secondary control level of the MG. In the design procedure, global variable feature of the MG frequency is taken into account to estimate the active power of the neighboring DGUs. Compared to the state of the art, the main contribution of the proposed control structure is that the SC is totally communication-free. Furthermore, straight-forward design, easy implementation, and consensus-based design to enhance the reliability of the system are the key features of the proposed SC. Experimental test, with four DGUs as a simplified MG, are carried on to validate the effectiveness of the proposed decentralized secondary control structure. The results show that the MG frequency is restored accurately, while the power is shared among DGUs by utilizing only local variables and with no communication network requirement. Future work will focus on extending the main ideas of this proposal to achieve a voltage control pattern with no need for communication infrastructure.

REFERENCES

[1] H. Bevrani, B. François, and T. Ise, *Microgrid dynamics and control*. John Wiley & Sons, 2017.

[2] R. Heydari, T. Dragicevic, and F. Blaabjerg, "High-bandwidth secondary voltage and frequency control of vsc-based ac microgrid," *IEEE Trans. Power Electron.*, vol. 34, no. 11, pp. 11 320–11 331, 2019.

[3] Q. Shafiee, V. Nasirian, J. C. Vasquez, J. M. Guerrero, and A. Davoudi, "A multi-functional fully distributed control framework for ac microgrids," *IEEE Trans. Smart Grid*, vol. 9, no. 4, pp. 3247–3258, 2018.

[4] T. Dragičević, R. Heydari, and F. Blaabjerg, "Super-high bandwidth secondary control of ac microgrids," in *APEC*. IEEE, 2018, pp. 3036–3042.

[5] F. Pasqualetti, F. Dörfler, and F. Bullo, "Attack detection and identification in cyber-physical systems," *IEEE Trans. Autom. Control*, vol. 58, no. 11, pp. 2715–2729, 2013.

[6] Y. Han, H. Li, P. Shen, E. A. A. Coelho, and J. M. Guerrero, "Review of active and reactive power sharing strategies in hierarchical controlled microgrids," *IEEE Trans. Power Electron.*, vol. 32, no. 3, pp. 2427–2451, 2017.

[7] Y. Han, K. Zhang, H. Li, E. A. A. Coelho, and J. M. Guerrero, "Mas-based distributed coordinated control and optimization in microgrid and microgrid clusters: A comprehensive overview," *IEEE Trans. Power Electron.*, vol. 33, no. 8, pp. 6488–6508, 2018.

[8] T. Dragicevic, D. Wu, Q. Shafiee, and L. Meng, "Distributed and decentralized control architectures for converter-interfaced microgrids," *Chinese J. Electr. Eng.*, vol. 3, no. 2, pp. 41–52, 2017.

[9] S. Liu, X. Wang, and P. X. Liu, "Impact of communication delays on secondary frequency control in an islanded microgrid." *IEEE Trans. Ind. Electron.*, vol. 62, no. 4, pp. 2021–2031, 2015.

[10] C. Ahumada, R. Cárdenas, D. Sáez, and J. M. Guerrero, "Secondary control strategies for frequency restoration in islanded microgrids with consideration of communication delays," *IEEE Trans. Smart Grid*, vol. 7, no. 3, pp. 1430–1441, 2016.

[11] E. A. A. Coelho, D. Wu, J. M. Guerrero, J. C. Vasquez, T. Dragicevic, C. Stefanovic, and P. Popovski, "Small-signal analysis of the microgrid secondary control considering a communication time delay." *IEEE Trans. Ind. Electron.*, vol. 63, no. 10, pp. 6257–6269, 2016.

[12] R. Heyderi, A. Amiri, T. Dragicevic, P. Popovski, and F. Blaabjerg, "High bandwidth distributed secondary control with communication compensation in vsc-based microgrid," in *2018 20th European Conference on Power Electronics and Applications (EPE'18 ECCE Europe)*. IEEE, 2018, pp. P–1.

[13] Q. Shafiee, Č. Stefanović, T. Dragičević, P. Popovski, J. C. Vasquez, and J. M. Guerrero, "Robust networked control scheme for distributed secondary control of islanded microgrids," *IEEE Trans. Ind. Electron.*, vol. 61, no. 10, pp. 5363–5374, 2014.

[14] J. W. Simpson-Porco, Q. Shafiee, F. Dörfler, J. C. Vasquez, J. M. Guerrero, and F. Bullo, "Secondary frequency and voltage control of islanded microgrids via distributed averaging." *IEEE Trans. Ind. Electron.*, vol. 62, no. 11, pp. 7025–7038, 2015.

[15] J. Schiffer, F. Dörfler, and E. Fridman, "Robustness of distributed aver-

aging control in power systems: Time delays & dynamic communication topology," *Automatica*, vol. 80, pp. 261–271, 2017.

[16] J. W. Simpson-Porco, F. Dörfler, and F. Bullo, "Synchronization and power sharing for droop-controlled inverters in islanded microgrids," *Automatica*, vol. 49, no. 9, pp. 2603–2611, 2013.

[17] A. Bidram, A. Davoudi, F. L. Lewis, and Z. Qu, "Secondary control of microgrids based on distributed cooperative control of multi-agent systems," *IET Gener. Transm. Dis.*, vol. 7, no. 8, pp. 822–831, 2013.

[18] A. Bidram, A. Davoudi, and F. L. Lewis, "A multiobjective distributed control framework for islanded ac microgrids," *IEEE Trans. Ind. Informat.*, vol. 10, no. 3, pp. 1785–1798, 2014.

[19] F. Dörfler, J. W. Simpson-Porco, and F. Bullo, "Breaking the hierarchy: Distributed control and economic optimality in microgrids," *IEEE Trans. Control Netw. Syst.*, vol. 3, no. 3, pp. 241–253, 2016.

[20] C. Li, E. A. A. Coelho, T. Dragicevic, J. M. Guerrero, and J. C. Vasquez, "Multiagent-based distributed state of charge balancing control for distributed energy storage units in ac microgrids," *IEEE Trans. Ind. Appl.*, vol. 53, no. 3, pp. 2369–2381, 2017.

[21] J. Schiffer, E. Fridman, R. Ortega, and J. Raisch, "Stability of a class of delayed port-hamiltonian systems with application to microgrids with distributed rotational and electronic generation," *Automatica*, vol. 74, pp. 71–79, 2016.

[22] X. Ge and Q.-L. Han, "Distributed formation control of networked multi-agent systems using a dynamic event-triggered communication mechanism," *IEEE Trans. Ind. Electron.*, vol. 64, no. 10, pp. 8118–8127, 2017.

[23] W. Heemels, K. H. Johansson, and P. Tabuada, "An introduction to event-triggered and self-triggered control," in *Decision and Control (CDC), IEEE 51st Annu. Conf. on*. IEEE, 2012, pp. 3270–3285.

[24] W. Heemels, R. Postoyan, M. Donkers, A. R. Teel, A. Anta, P. Tabuada, and D. Nešic, "Periodic event-triggered control," *Event-based control and signal processing*, pp. 105–119, 2015.

[25] Y. Khayat, M. Naderi, Q. Shafiee, M. Fathi, H. Bevrani, T. Dragicevic, and F. Blaabjerg, "Communication-less optimal frequency control of islanded microgrids," in *EPE'18 ECCE Europe*. IEEE, 2018, pp. 1–8.

[26] Y. Khayat, M. Naderi, Q. Shafiee, Y. Batmani, M. Fathi, J. M. Guerrero, and H. Bevrani, "Decentralized optimal frequency control in autonomous microgrids," *IEEE Transa. Power Syst. , DOI: 10.1109/TPWRS.2018.2889671.*, 2018.

[27] M. Naderi, Y. Khayat, Q. Shafiee, T. Dragicevic, F. Blaabjerg, and H. Bevrani, "An emergency active and reactive power exchange solution for interconnected microgrids," *IEEE Journal of Emerg. Sel. Topics Power Electron.*, 2019.

[28] Y. Khayat, R. Heydari, M. Naderi, T. Dragicevic, Q. Shafiee, M. Fathi, H. Bevrani, and F. Blaabjerg, "Estimation-based consensus approach for decentralized frequency control of ac microgrids," in *2019 21st European Conference on Power Electronics and Applications (EPE'19 ECCE Europe)*. IEEE, 2019, pp. 1–8.

[29] M. Yazdanian and A. Mehrizi-Sani, "Washout filter-based power sharing." *IEEE Trans. Smart Grid*, vol. 7, no. 2, pp. 967–968, 2016.

[30] Y. Han, H. Li, L. Xu, X. Zhao, and J. M. Guerrero, "Analysis of washout filter-based power sharing strategyan equivalent secondary controller for islanded microgrid without lbc lines," *IEEE Trans. Smart Grid*, vol. 9, no. 5, pp. 4061–4076, 2018.

[31] Y. Sun, X. Hou, J. Yang, H. Han, M. Su, and J. M. Guerrero, "New perspectives on droop control in ac microgrid," *IEEE Trans. Ind. Electron.*, vol. 64, no. 7, pp. 5741–5745, 2017.

[32] J. Lu, M. Savaghebi, and J. M. Guerrero, "Second order washout filter based power sharing strategy for uninterruptible power supply," in *Ind. Electron. Soc., IECON 43rd Annu. Conf. of the IEEE*. IEEE, 2017, pp. 7854–7859.

[33] W. Gu, G. Lou, W. Tan, and X. Yuan, "A nonlinear state estimator-based decentralized secondary voltage control scheme for autonomous microgrids," *IEEE Trans. Power Syst.*, vol. 32, no. 6, pp. 4794–4804, 2017.

[34] G. Lou, W. Gu, L. Wang, B. Xu, M. Wu, and W. Sheng, "Decentralised secondary voltage and frequency control scheme for islanded microgrid based on adaptive state estimator," *IET Gener. Transm. Dis.*, vol. 11, no. 15, pp. 3683–3693, 2017.

[35] J. M. Rey, P. Martí, M. Velasco, J. Miret, and M. Castilla, "Secondary switched control with no communications for islanded microgrids," *IEEE Trans. Ind. Electron.*, vol. 64, no. 11, pp. 8534–8545, 2017.

[36] W. Liu, W. Gu, W. Sheng, X. Meng, Z. Wu, and W. Chen, "Decentralized multi-agent system-based cooperative frequency control for autonomous microgrids with communication constraints," *IEEE Trans. Sustainable Energy*, vol. 5, no. 2, pp. 446–456, 2014.

[37] C. Dou, M. Lv, T. Zhao, Y. Ji, and H. Li, "Decentralised coordinated control of microgrid based on multi-agent system," *IET Gener. Transm. Dis.*, vol. 9, no. 16, pp. 2474–2484, 2015.

[38] Q. Li, F. Chen, M. Chen, J. M. Guerrero, and D. Abbott, "Agent-based decentralized control method for islanded microgrids," *IEEE Trans. Smart Grid*, vol. 7, no. 2, pp. 637–649, 2016.

[39] Y. Khayat, Q. Shafiee, R. Heydari, M. Naderi, T. Dragicevic, J. W. Simpson-Porco, F. Dorfler, M. Fathi, F. Blaabjerg, J. M. Guerrero *et al.*, "On the secondary control architectures of ac microgrids: An overview," *IEEE Trans. Power Electron.*, 2019.

[40] F. Milano, F. Dörfler, G. Hug, D. J. Hill, and G. Verbič, "Foundations and challenges of low-inertia systems," in *2018 Power Systems Computation Conference (PSCC)*. IEEE, 2018, pp. 1–25.

[41] H. Bevrani, *Robust power system frequency control*. 2nd Ed., Springer, 2014.

[42] R. Olfati-Saber, J. A. Fax, and R. M. Murray, "Consensus and cooperation in networked multi-agent systems," *Proceedings of the IEEE*, vol. 95, no. 1, pp. 215–233, 2007.

[43] H. Zhang, F. L. Lewis, and Z. Qu, "Lyapunov, adaptive, and optimal design techniques for cooperative systems on directed communication graphs," *IEEE Trans. Ind. Electron.*, vol. 59, no. 7, pp. 3026–3041, 2012.

[44] M. Naderi, Y. Khayat, Q. Shafiee, H. Bevrani, and F. Blaabjerg, "Modeling of islanded microgrids using static and dynamic equivalent thevenin circuits," in *EPE'18 ECCE Europe*. IEEE, 2018, pp. 1–10.

[45] Q. Shafiee, J. M. Guerrero, and J. C. Vasquez, "Distributed secondary control for islanded microgridsa novel approach," *IEEE Trans. Power Electron.*, vol. 29, no. 2, pp. 1018–1031, 2014.